Kurdish Studies
Feb 2024
Volume: 12, No: 2, pp.227-236
ISSN: 2051-4883 (Print) | ISSN 2051-4891 (Online)
www.KurdishStudies.net

Received: December 2023 Accepted: January 2024
DOI: https://doi.org/10.58262/ks.v12i2.019

Laser-induced Surface Modifications for Hydrophilicity and Hydrophobicity Applications

A. A. Hatem[1]*, B. G. Rasheed[1]

Abstract

Surface reconstruction for various materials was performed using lasers devoted for hydrophilic and hydrophobic applications. Photoelectrochemical etching of Silicon using diode laser of 532 nm was carried out to synthesize nanostructured layer with contact angles varied from (70°) to (115°) according to the preparation conditions. This process produces hydrophobic surfaces. While fiber laser of 1064 nm wavelength was employed for surface micro texturing of glass and stainless steel. Hereby, hydrophilic effect was observed.with contact angles in the ranges (10°-35°) and (14°-74°) for glass and stainless steel, respectively. Morover, Superhydrophilic surfaces with minimum contact angles (10°) and (14°) for both glass and stainless steel respectively when silicon nanoparticles of average size (10 nm) embedded in microstructured surfaces. It is also found that large surface area of Silicon surface leads to increase the contact angle.

Keywords: *Silicon Nanostructure, Silicon Microstructure. Hydrophobic, Hydrphpilic.*

Introduction

The wettability of material surfaces are crucial in determining the nature of fluid-surface interactions[1]. The phenomenon of wetting behavior is seen everywhere. However, it exhibits a distinct and intriguing variability [2].

In a scenario characterized by non-wetting conditions, water exhibits unhindered mobility as it rolls over the external surface of the leaf. The water droplet has a nearly spherical morphology, facilitating its rolling motion. This feature presents a self-cleansing characteristic, as the presence of impurities may be effectively eliminated by the action of the rolling drop [3-4]. The observed phenomenon is characterized by an anisotropic non-wetting condition, facilitating the preferential rolling of water droplets along the longitudinal direction of the surface rather than the perpendicular direction [5].

For a long time, the terms "hydrophilic surface" and "hydrophobic surface" have been used extensively in literature. These phrases denote contrasting phenomena of the interaction between water and a solid surface. Hydrophilic surfaces display a strong affinity for water molecules, while hydrophobic surfaces have the capability to repel water [6].

A primary indicator for categorising fluid-wetting behaviour as hydrophilic or hydrophobic is the measurement of the contact angle [7]. At the point where a liquid meets a solid or a vapour, an angle is formed; this angle is called the contact angle. Hydrophilic materials are those with

[1] Laser &Optoelectronics Engineering Department, College of Engineering, Al-Nahrain University, Baghdad, Iraq.
*Corresponding author: Email: aarafalsarah@gmail.com

a contact angle (θe) below 90°, hydrophobic materials have a contact angle ranging from 90° to 150°, and super-hydrophobic materials have a contact angle exceeding 150°. This is how materials are classified based on their water droplet contact angles. A substance's hydrophobicity is enhanced when the contact angle increases, which is correlated with a stronger liquid-liquid interaction [8-10].

Numerous industries, including healthcare and electronics, make use of surface treatment technologies. Wettability characteristics in materials can be altered by modifying both their chemical and physical characteristics, leading to modifications in their wetting capabilities [11].

Hydrophilic and hydrophobic materials play a crucial role in the process of separating oil and water, especially when considering environmental and energy factors [12]. The study of wetting and spreading phenomena seen in natural systems has garnered significant attention, primarily because of the extensive range of potential applications associated with this phenomenon.

The objective of this study is to investigate hydrophilic and hydrophobic surfaces and how microstructured surfaces properties can be alterd from one property to another.

The Experimental Work

Various approaches were employed to fabricate micro/nano-structures on silicon wafers, glass slides, and stainless steel surfaces, resulting in surfaces that exhibit either hydrophilic or hydrophobic properties.

To create micro/nano structures forsilicon, laser texturing and photo-electrochemical etching were applied. Nanostructured layer was created by photo-electrochemical etching [12]. In a Teflon cell, silicon (Si) wafers were completely submerged in a 40% hydrofluoric (HF) acid solution. The wafers were subsequently subjected to 20 minutes of photo-electrochemical etching, as illustrated in Fig. (1), using a diode laser irradiation at wavelength of 532 nm and power density of 5 W/cm^2. The etching current densities spanned from 5 to 20 mA/cm^2 and the laser spot diameter of 1 cm. Additionally, it is worth to notice that the backside of the wafer was well isolated from the etching acid.Compared to the bandgap energy of silicon (1.12 eV), the photon energy of the laser under consideration is (2.33 eV), almost twice as high. Consequently, this laser is appropriate for photo-electrochemical etching due to its enhanced photo-absorption capabilities [13]. AFM analysis was also used to investigate the nanostructured silicon surfaces.

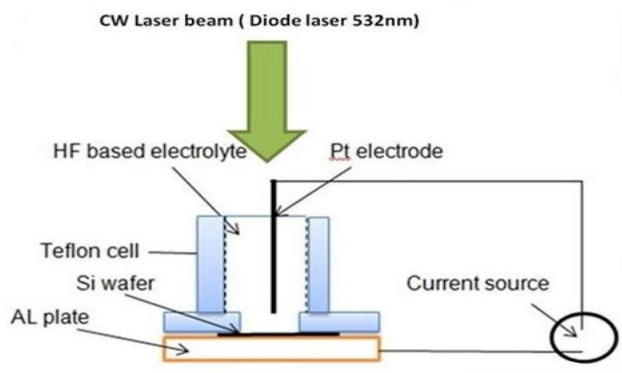

Figure (1): The Experimental Setup for Photo-electrochemical Etching by Diode Laser.

Microstructures were produced on the surface of silicon wafers, glass slides, and stainless steel sections through the use of laser surface texturing. This was accomplished by employing a fibre laser with a wavelength of (1064 nm), a pulse duration of (127 ns), a frequency of (10 Hz), and intensity ranging from (1-30 W). The laser system equipped with a scanning optical system and (f θ) lens. The experimental setup for laser texturing is shown in Figure 2.

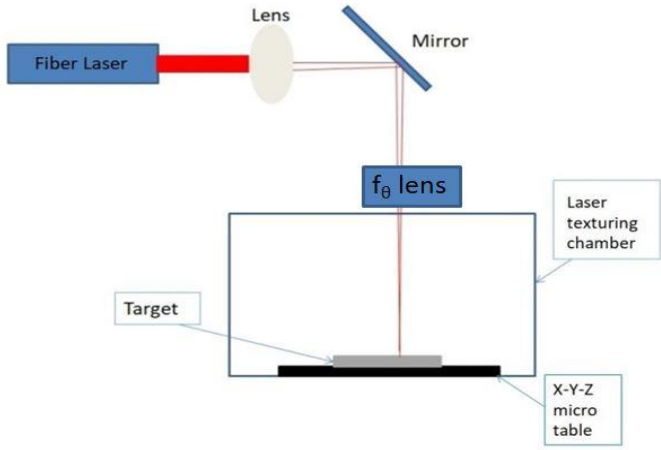

Figure (2): The Experimental Setup For Laser Texturing by Fiber Laser.

Moreover, laser ablation in liquid shown in fig. (3) was also used for synthesis silicon micro/ nano particles. The laser was set to hit Si target with Nd:YAG laser of pulse duration (10 ns). Then, the suspension was subjected to fiber laser with a high repetition rate of 30 KHz, for 15 minutes to produce silicon nanoparticles by laser fragmentation process.

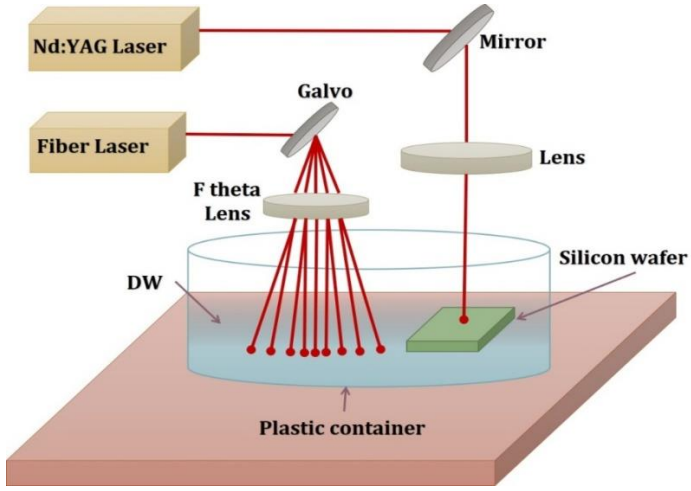

Figure (3): The Experimental Setup For Laser Ablation By Nd:YAG Laser.

The microstructure of the glass and stainless steel surfaces was examined using a high-resolution optical microscope supported with a digital camera (OLYMPUS BX60M). The contact angle was then analyzed and measured using optical image software (imagej).

Results And Discussion

The silicon surface was reconstructed by the use of photo-electrochemical etching by diode laser. While glass and stainless steel surfaces were reconstructed through the use of laser texturing with fiber laser. Figure 4 displays the profile of a water droplet on a smooth surface made of silicon, glass, and stainless steel.

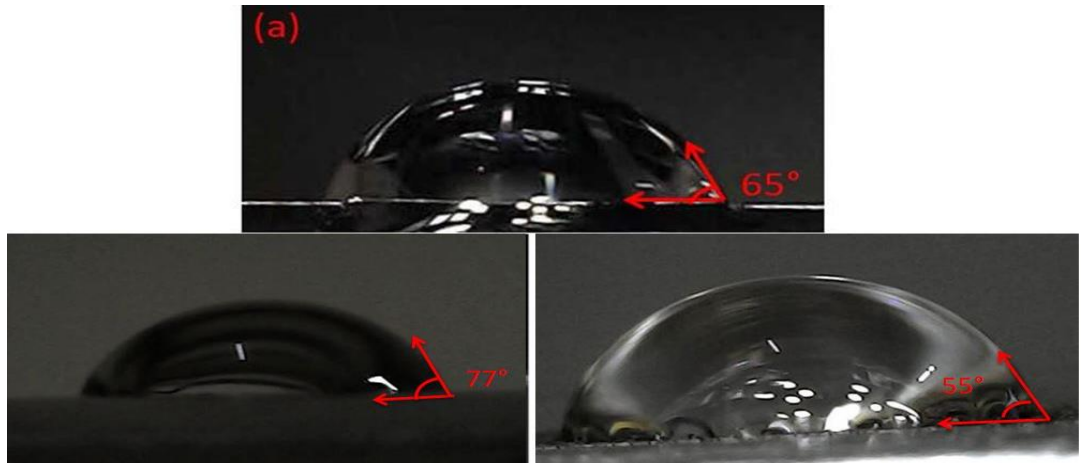

Figure (4): The Water Droplet Upon the Bare Surfaces of:a) Silicon, B) Glassand C) Stainless Steel.

Nanostructured silicon surfaces with a variety of morphologies have been created by photo-electrochemical etching process, while the laser texturing method can produce microstructured silicon structures.

Figure 5 shows the contact angle of Si nano-surfaces for n-type which is higher than that for p-type.

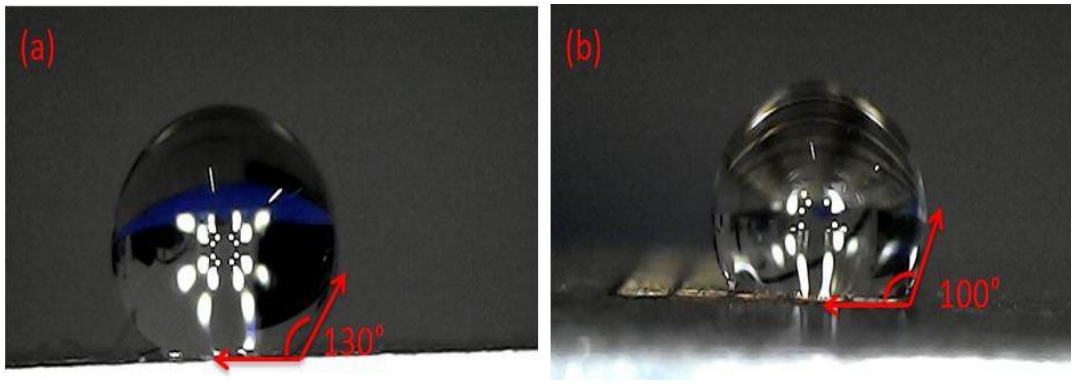

Figure (5): The Water Droplet Upon of Silicon Surface for:a) N-type and B) P-type.

AFM was also used to analyze the nanostructured layer that was formed on the silicon surface by photoelectrochemical etching with diode laser. Figure 6 show the nanostructured surface morphology of n-type and p-type silicon substrates with their corresponding histograms for the two substrates. The histograms illustrate the generation of a uniform Gaussian size distribution, with an average size of 150 nm for n-type silicon and 90 nm for p-type silicon.

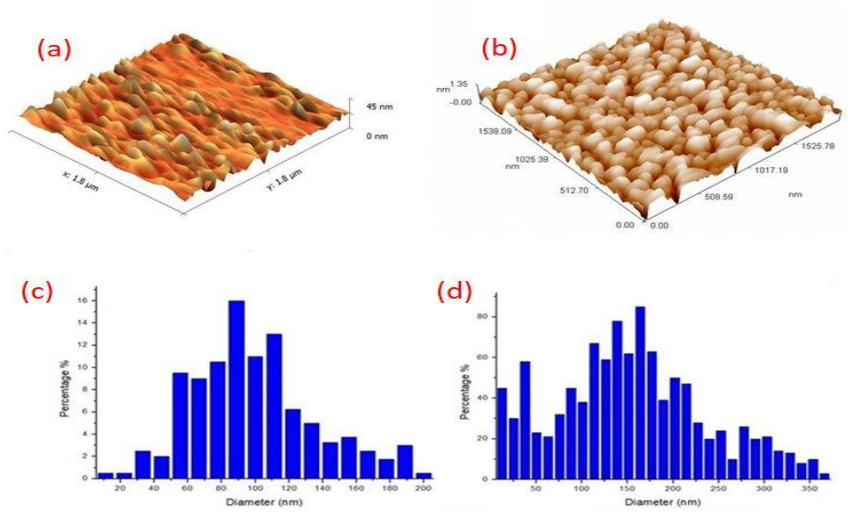

Figure (6): the Afm Images and the Corresponding Histogram of (a & C) N-typesi and (B & D) P-type Si.

It is found that the contact angle for bare silicon surface was 65°. While for the nanostructured surface of n-type silicon surface, the contact angle was 130° after photo-electrochemical etching, whereas for p-type silicon surface, this angle was 100°. This is attributed to the size reduction due to the dissolution in n-type silicon by photo-electrochemical etching because of the photo generated holes compared with that for p-type silicon. The calculated surface area reveals a remarkable increment for smaller nanostructured surfaces with relatively greater contact angles. The increased potential adsorption for a larger surface area is responsible for this phenomenon. Because of this, the water droplet is pushed up by the silicon nanostructured surface as a result of the adsorption action, and the surface is then found to be hydrophobic.

Table (1): The Silicon Surface With Contact Angle for N and P-type for Different Average Sizes.

	Average size (nm)	**Contact angle (°)**	**Surface area($\frac{m^2}{m^3}$)**
n-type Silicon	Bare	65	3.8$m\mathrm{m}^2$
	200	85	290
	150	100	348
	100	115	388
	50	130	390
p-type Silicon	Bare	65	3.8mm^2
	200	70	136
	150	80	264
	100	90	296
	50	100	350

Differently, the process of laser texturing with fiber laser leads to the formation of microstructures on the surface of silicon wafers with variable line widths, ranging from 50 to 300 µm.

Table 2 gives the contact angles between silicon surface produced by laser texturing and water droplet. It explains that the contact angles of smaller microstructures dimensions are lower.The smaller surface area of these structures is probably the cause of this. Therefore, the microstructured silicon surface and water droplet have a stronger adsorption effect. Accordingly, the silicon wafer's surface undergoes a transition to a state of superhydrophobicity.

Table (2): The Bare and Micro Textured Silicon Surfaces Contact Angle and Surface Area.

Micro structure(μm)	Contact angle(°)	Surface area($\frac{\mathbf{m^2}}{\mathbf{m^3}}$)
Bare	65	$3.8mm^2$
50	8	144
100	11	168
150	13	180
200	15	196
250	17	217
300	20	250

Laser texturing employs the feeble absorption of the fiber laser wavelength by glass, thereby enabling the formation of microstructures. The microstructure dimensions demonstrate an exceptional degree of hydrophilicity.Therefore, silicon nanoparticles generated via Nd:YAG laser ablation were incorporated into the glass microstructure in order to impart a hydrophobic surface, should the need arise for such a characteristic.

The embedding of silicon nanoparticles with an average size of 220 nm, as illustrated in figure 7, within glass microstructures has been observed to result in increased contact angles.

In addition, silicon nanosuspension was generated by Nd:YAG laser under subsequent fiber laser fragmenting. Extremely smaller silicon nanoparticles were created by this process. As illustrated in figure 7, silicon nanoparticles have of average size 10 nm were formed. These nanoparticles could increase the surfafe area of the microstructure dimensions.

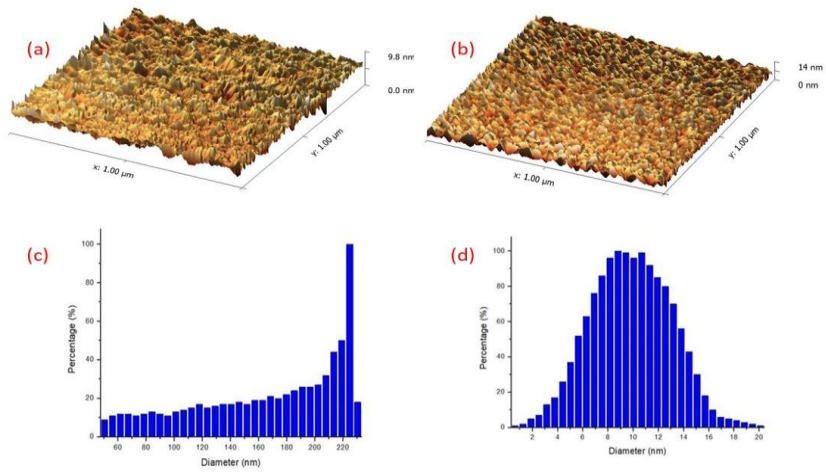

Figure (7): The Afm Image and the Corresponding Histogram for the Si Nanoparticles of (a, C) Before Fragmentation and (B, D) After Fragmentation.

Several attempts were carried out to convert a hydrophilic glass surface to hydrophobic surface are detailed in Table 3. These attempts include adding Si nanoparticles of varying sizes to the glass surface's microstructure and widening the lines. The contact angles of glass microstructures with and without silicon nanoparticles are presented in Table 3.
In the absence of silicon nanoparticles, glass demonstrates hydrophilic properties and possesses a contact angle of 35°. The contact angle increases to 40° when silicon nanoparticles produced via laser ablation with Nd: YAG are incorporated into the microstructured surface.Then, the contact angle increases to 52° when silicon nanoparticles produced by fragmentation with a fiber laser are incorporated into the micro structured glass surface, as shown in Figure 8.

Table (3): The Contact Angle Between the Water Droplet and the Glass Surface With and Without Si Nanoparticles.

Glass (μm)	Surface area($\frac{m^2}{m^3}$)	CA (°)	CA (°) With Si-nanoparticles	CA (°) With Si-nanoparticles after fragmentation
Bare	$4.8m^2$	55	/	/
50	111	10	15	22
100	122	12	19	30
150	163	14	24	33
200	177	16	29	37
250	189	23	33	44
350	211	30	36	45
500	240	35	40	52

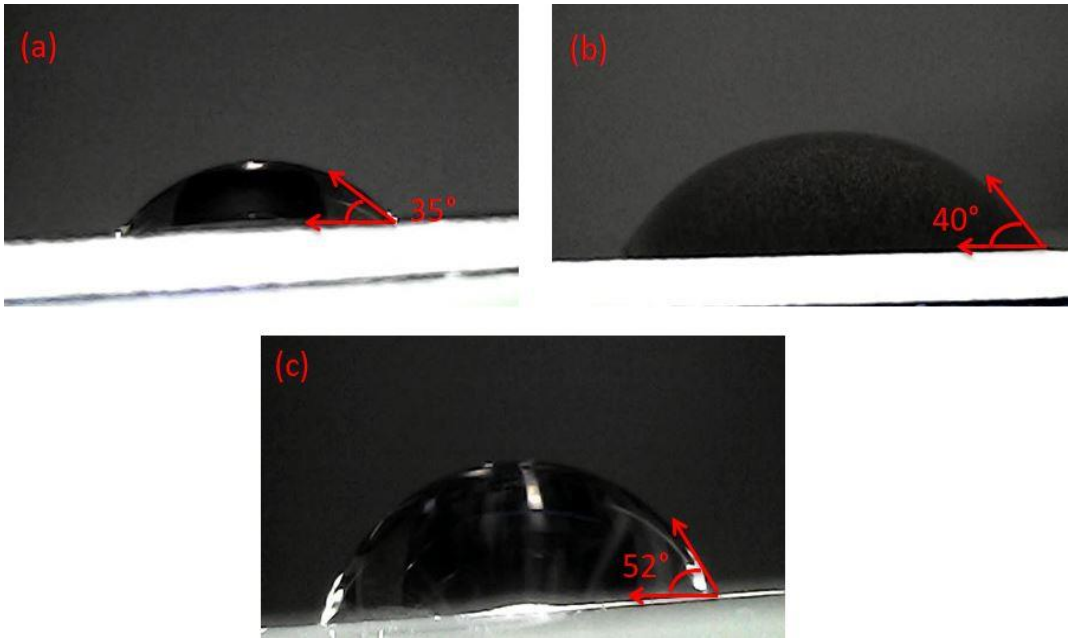

Figure (8): The Water Droplet Upon the Surfaceof Glass for:a) Microstructure, B) Microstructure With Si Nanoparticles and C) Microstructure With Si Nanoparticles.

Moreover, microstructured surface for stainless steel was produced by laser texturing of stainless-steel surfaces using fiber laser.

The present study investigates the microstructures formed on the laser-ablated surface of stainless steel, where line spacing differs between 150 and 450 μm were created. Table 4 presents the contact angle measurements of a water droplet on surfaces that have been treated (ablated) for both prior to and subsequent to the introduction of Si nanoparticles.

This result demonstrates the effect that increasing line breadth (the microstructure dimension) and incorporating nanoparticles into the microstructure have increase the surface area and contact angle.The contact angle exhibits an increase with the addition of Si nanoparticles and further increase when smaller nanoparticles reduced by laser fragmentationare embedded into the surface. This observation shows a hydrophobic property exhibited by the treated surface.

Table (4): The Contact Angle for the Stainless Steel Surface Befors and After Adding Si Nanoparticles.

Microstructure Dimension (μm)	**Surface area($\frac{m^2}{m^3}$)**	**Contact angle (°)**		
		Without Si NPs	Si NPs before fragmentation	Si NPs after fragmentation
Bare	$2.5m^2$	77	/	/
150	179	20	45	75
250	151	31	51	87
350	112	42	68	100
450	104	70	75	120

Figure 9 illustrates the contact angles before and after adding silicon nanoparticles on the stainless steel surface.

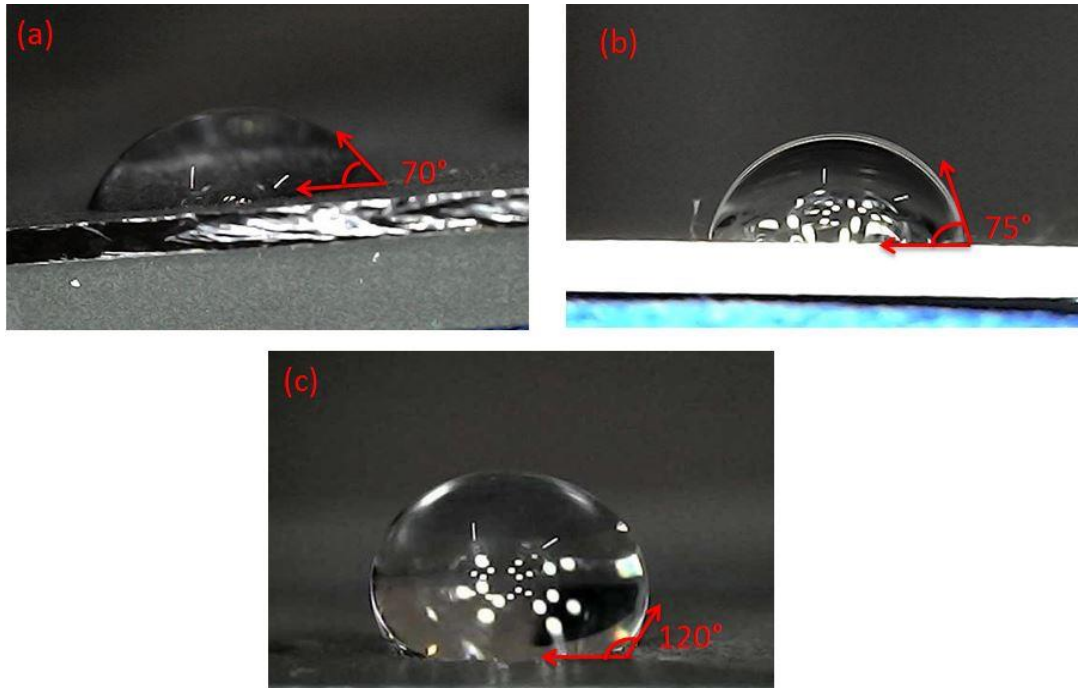

Figure (9): The Water Droplet Upon the Surfaceof Stainless Steel for:a) Microstructure, B) Microstructure With Si Nanoparticles and C) Microstructure With Smalleer Si Nanoparticles.

Effect of aging time on the contact angle for stainless steel microstructure was also examined. Table 5 explains the impact of time on the contact angle for microstructured stainless steel surface. The contact angles between the water droplet and the laser-textured surface exhibit decreased values. The contact angle progressively rises over time as the surface undergoes oxidation [14].

Table (5): The Contact Angle Between the Water Droplet and the Stainless Steel Surface With Time.

Microstructure Dimension (μm)	**Contact angle (°)**		
	Fresh	After 2 weeks	After 2 months
Bare	77	/	/
150	20	47	110
250	31	55	120
350	42	61	135
450	70	90	160

Conclusions

Many potential applications depend on the Surface properties. Nanostructured Silicon surface synthesized by diode laser using photoelectrochemical etching. This process exihibts hydrophobic surface with contact angles greater than 90 degree. While microstructured surfaces for glass and stainless steel were produced by laser texturing using fiber laser. Hydrophilic surfaces for both materials was observed. These hydrophilic surface can be converted to hydrophobic if it is nedded when Silicon nanparticles embedded at those surfaces. Aging time of microstructured stainless steel surface leads to increase the contact angles of water sroplet due to the oxidation effect.

Reference

1. Tarek, Ahmed. Chapter 4 - Fundamentals of Rock Properties. Reservoir Engineering Handbook (Fifth Edition). Gulf Professional Publishing. (2019). 167-281.
2. Bonn, D., J. Eggers, J. Indekeu, J. Meunier, and E. Rolley. Wetting and spreading. Reviews of Modern Physics. 81: (2009) 739–805.
3. Barthlott, W., and C. Neinhuis. Purity of the sacred lotus, or escape from contamination in biological surfaces. Planta (1997)202:1–8.
4. Yu, C.; Liu, M.; Zhang, C.; Yan, H.; Zhang, M.; Wu, Q.; Liu, M.; Jiang, L. Bio-Inspired Drag Reduction: From Nature Organisms to Artificial Functional Surfaces. Giant (2020), 2, 100017.
5. Wu, D., J.-N. Wang, S.-Z. Wu, Q.-D. Chen, S. Zhao, H. Zhang, et al. Three-level biomimetic rice-leaf surfaceswith controllable anisotropic sliding. Advanced Functional Materials 21: (2011) 2927–32.
6. Drelich, J., E. Chibowski, D. D. Meng, and K. Terpilowski. Hydrophilic and superhydrophilic surfaces andmaterials. Soft Matter 7: (2011) 9804.
7. Puntervold, T., Strand, S., Mamonov, A., & Piñerez, I. D. T. Enhanced oil recovery by Smart Water injection in sandstone reservoirs. In Recovery Improvement (2023) (pp. 109-184). Gulf Professional Publishing.
8. Tae Oh Yoon, Hyun Joo Shin, Sae ChaeJeoung, and Youn-Il Park, "Formation of superhydrophobic poly(dimethysiloxane) by ultrafast laser-induced surface modification," Opt. Express 16, (2008) 12715-12725.

9. Ganesan, P., S. M. Vanaki, K. K. Thoo, and W. M. ChinAir-side heat transfer characteristics of hydrophobicand super-hydrophobic fin surfaces in heat exchangers: A review. International Communicable Heat MassachusettsTransf 74:27–35 (2016).
10. SlepickovaKasalkova, N., Slepicka, P., Kolska, Z., &Svorcik, V. (2015). Wettability and Other Surface Properties of Modified Polymers. InTech.
11. Chu, Z., Y. Feng, and S. Seeger. Oil/water separation with selective superantiwetting/superwetting surface materials. AngewChemie International Editors 54: (2015) 2328–38.
12. Rasheed BG. Synthesis of silicon nanostructures: comparative study. Advances in Materials.;2(1) (2013) 6-11.
13. Badriyah Alhalaili, Ruxandra Vidu, Howard Mao, Olfa Kamoun, M. Saif Islam. Photoelectrochemical (PEC) etching of Ga2O3. Ceramics International, Volume 47, Issue 1, (2021) Pages 479-486.
14. Al-Ameer MA, Azad MS, Al-Shehri D, Mahmoud M, Kamal MS, Patil S. A Guide for Selection of Aging Time and Temperature for Wettability Alteration in Various Rock-Oil Systems. ACS Omega. 16;8(34) (2023) 30790-30801.